

Early-Time Symmetry Tuning in the Presence of Cross-Beam Energy Transfer in ICF Experiments on the National Ignition Facility

E. L. Dewald,¹ J. L. Milovich,¹ P. Michel,¹ O. L. Landen,¹ J. L. Kline,² S. Glenn,¹ O. Jones,¹ D. H. Kalantar,¹ A. Pak,¹ H. F. Robey,¹ G. A. Kyrala,² L. Divol,¹ L. R. Benedetti,¹ J. Holder,¹ K. Widmann,¹ A. Moore,¹ M. B. Schneider,¹ T. Döppner,¹ R. Tommasini,¹ D. K. Bradley,¹ P. Bell,¹ B. Ehrlich,¹ C. A. Thomas,¹ M. Shaw,¹ C. Widmayer,¹ D. A. Callahan,¹ N. B. Meezan,¹ R. P. J. Town,¹ A. Hamza,¹ B. Dzenitis,¹ A. Nikroo,³ K. Moreno,³ B. Van Wonterghem,¹ A. J. Mackinnon,¹ S. H. Glenzer,¹ B. J. MacGowan,¹ J. D. Kilkenny,¹ M. J. Edwards,¹ L. J. Atherton,¹ and E. I. Moses¹

¹Lawrence Livermore National Laboratory, Post Office Box 808, Livermore, California 94550, USA

²Los Alamos National Laboratory, Los Alamos, New Mexico 87545, USA

³General Atomics, San Diego, California 92186, USA

(Received 26 February 2013; published 2 December 2013)

On the National Ignition Facility, the hohlraum-driven implosion symmetry is tuned using cross-beam energy transfer (CBET) during peak power, which is controlled by applying a wavelength separation between cones of laser beams. In this Letter, we present early-time measurements of the instantaneous soft x-ray drive at the capsule using reemission spheres, which show that this wavelength separation also leads to significant CBET during the first shock, even though the laser intensities are $30\times$ smaller than during the peak. We demonstrate that the resulting early drive P_2/P_0 asymmetry can be minimized and tuned to $<1\%$ accuracy (well within the $\pm 7.5\%$ requirement for ignition) by varying the relative input powers between different cones of beams. These experiments also provide time-resolved measurements of CBET during the first 2 ns of the laser drive, which are in good agreement with radiation-hydrodynamics calculations including a linear CBET model.

DOI: [10.1103/PhysRevLett.111.235001](https://doi.org/10.1103/PhysRevLett.111.235001)

PACS numbers: 52.57.Fg, 52.38.-r

Capsule tuning experiments on the National Ignition Facility (NIF) [1] using 192 laser beams, with total energy ranging between 1 and 2 MJ, have been under way since 2009 [2]. Their goal is to optimize the compression of a deuterium-tritium (DT)-filled, 2-mm diameter capsule embedded in a cm-long cryogenic He-filled high- Z cylindrical “hohlraum” [3,4] in an attempt to bring it to ignition and burn [5]. In order to achieve the required implosion symmetry, the laser beam spots at the wall are arranged in three rings, each consisting of 64 laser beams, with nearly uniform azimuthal wall coverage: the “inner” ring, located near the hohlraum midplane, and the two “outer” rings, each arranged symmetrically above and below the midplane. Thus, whereas the odd Legendre polynomials (P_1, P_3, \dots) of the flux incident onto the capsule are intrinsically small and mainly due to random power imbalances of the laser beams [6,7], the low order even modes (P_2, P_4) need to be minimized by hohlraum geometry, relative cone powers, and beam pointing [2,8].

In order to achieve sufficient compression of the DT fuel, a carefully tailored sequence of four shock waves is launched into the target using a laser pulse that incorporates four successive steps in power [9] [cf. Fig. 1(a)]. Radiation-hydrodynamics simulations [10] have shown that the shape of the capsule at ignition time is mainly sensitive to radiation asymmetries occurring during the first pulse [the “picket,” at $t \sim 0\text{--}2$ ns in Fig. 1(a)] and the fourth pulse ($t \sim 20$ ns). In principle, the control of the P_2 drive flux at

the capsule could be achieved by tuning the incident laser cone fraction (the ratio of inner beam power to total power). However, during the fourth pulse, at peak laser powers relevant for ignition, the incident cone fraction is limited by the power and energy thresholds of the NIF laser system to 0.33 (i.e., the same peak power in all the beams). For this reason the fourth pulse radiation nonuniformities are controlled by cross-beam energy transfer (CBET) [11–13]. CBET effectively modifies the laser cone fraction at the hohlraum wall while keeping the input laser power fixed, thus allowing for time-integrated symmetric drive. This scheme, where diffraction gratings are imprinted in the plasma via the ponderomotive force of the beat waves between crossing laser beams, is tunable by independently setting the wavelengths of different cones of laser beams.

Mitigation of the radiation flux asymmetries in the picket is also needed, since they are responsible for time-dependent swings of the low-order modes during the final compression of the capsule, which can lead to unacceptable levels of shell and hot spot deformation [14]. In addition, drive flux asymmetries are tantamount to nonuniformities in shock velocity and timing, which produce local increases in hot-spot entropy. This effect is particularly important during the picket, which sets the arrival time and the strength of the first shock at the inner surface of the DT fuel, largely determining the implosion adiabat [15].

In this Letter, we report on high precision measurements and control of the radiation flux symmetry during the

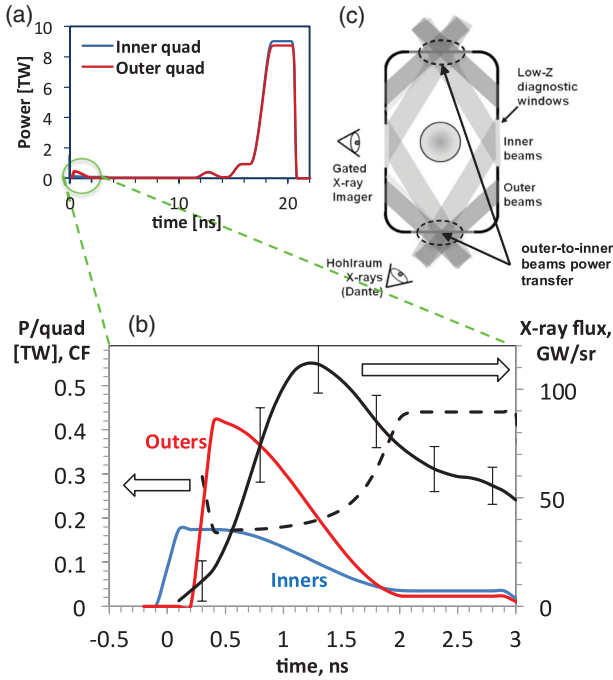


FIG. 1 (color). (a) Full NIF pulse shape for an inner and an outer quadruplet of laser beams (“quad”); the maximum total power from the 48 NIF quads is 420 TW; (b) zoom in on the picket (first pulse), showing the incident power per quad, cone fraction (black dash) and hohlraum x-ray flux measured by Dante (black solid) in a scale 544 hohlraum. (c) Setup of reemit experiments on the NIF.

picket of a NIF ignition pulse. By matching the time-resolved P_2 symmetry between experiments with ($\Delta\lambda \neq 0$) and without CBET ($\Delta\lambda = 0$), we infer the level of CBET without relying on numerical simulations. These also represent the first time-resolved measurement of CBET in an ignition hohlraum. The results are in good agreement with calculations from the radiation-hydrodynamics code HYDRA [16] coupled to a linear model of CBET [12,17], which show a linear amplification of the inner beams by more than a factor of 2 in the picket for $\Delta\lambda = 1.8 \text{ \AA}$. Unlike CBET during the fourth pulse, studied before [11–13], CBET in the picket is in a linear and unsaturated regime due to differences in hohlraum fill plasma conditions.

The measurement of the picket radiation drive symmetry in NIF ignition hohlraums is performed using the reemit technique [18]. The experimental layout is shown in Fig. 1(c), in which the ignition capsule is replaced with a high-Z sphere of similar dimensions. The symmetry of the incoming flux at the capsule is inferred by measuring the soft x-ray reemission pattern at the limb of the sphere. The target design uses a $\sim 2 \text{ mm}$ diameter Bi capsule mounted in a He gas-filled (0.96 mg/cc) gold hohlraum with two 2.7 mm diameter diagnostic holes, which are covered with $1 \text{ }\mu\text{m}$ thick polyimide windows that allow soft x-ray imaging and reduce background signal from the

backside wall emission. Data were acquired at four independent times in the $0.9\text{--}2.2 \text{ ns}$ time interval using a 4-strip gated x-ray imager with 100 ps exposure time [19]. The hohlraum is heated by 351 nm wavelength ignition pulses terminated at 3 ns as shown in Fig. 1(b), which also shows a typical power cone fraction history, $CF(t) = P_{\text{inn}}(t) / [P_{\text{inn}}(t) + P_{\text{out}}(t)]$, where P_{inn} and P_{out} are the inner and outer beam powers, and $P_{\text{tot}} = P_{\text{inn}} + P_{\text{out}}$ is the total laser power. In the following, we will parametrize our tuning curves by using $CF_0 = CF(t = 0.5 \text{ ns})$ where the picket laser power is at a maximum.

Images are recorded in the high-energy ($h\nu$) tail of the sphere reemission Planckian spectrum. For an ideal Planckian, this leads to an enhancement factor $h\nu/4kT_{\text{re}}$ in the measured asymmetry relative to the asymmetry of the spectrally integrated radiation drive incident onto the capsule; k is the Boltzmann constant and T_{re} is the average reemission temperature of the sphere limb. For typical picket conditions, we calculate a reemission temperature $T_{\text{re}} \approx 65 \text{ eV}$ for an incoming x-ray drive temperature at the capsule of $T_r = 75 \text{ eV}$. Using different combinations of x-ray filters and imaging pinholes ($50, 100 \text{ }\mu\text{m}$ diameter), the diagnostic records images at two centroid photon energies (600 and 800 eV) each with a spectral width of $\sim 300 \text{ eV}$, representing enhancement factors of $h\nu/4kT_{\text{re}} = 2.3$ and 3.1 , respectively. Having two separate measurements at different energies enables a validation of the $h\nu/4kT_{\text{re}}$ factors and hence the inferred incident P_2/P_0 . This reduces the sensitivity to uncertainties in T_{re} and in deviations of the Bi reemission spectrum from an ideal Planckian. With this setup, the measured photon collection statistics, validated experimentally in previous vacuum hohlraum reemit experiments [20] performed at the OMEGA Laser Facility [21], translates to an inferred incident P_2/P_0 statistical accuracy of $\pm 1\%$.

To assess the sensitivity of the ignition capsule implosion performance to the picket P_2 asymmetry (CF) three-dimensional HYDRA simulations were performed, where the x-ray drive was artificially symmetrized for $t > 2.5 \text{ ns}$. The results, summarized in Fig. 2, indicate that to stay below an acceptable 10% yield degradation, $\Delta\langle\rho R\rangle < 10\%$, setting the picket symmetry requirement of $|P_2/P_0|$ at $< 7.5\%$ (blue box in Fig. 2).

Note that a specified picket symmetry reverses at ignition time; i.e., pole hot picket symmetry results in waist hot implosion and vice versa (insets in Fig. 2). Calculations also show an offset between reemit and ignition targets (Fig. 2). This can be explained by additional radiation losses through the diagnostic holes at the capsule waist for reemits, reducing the effective cone fraction at the wall. These losses and the differences between capsule and reemit sphere x-ray albedos give a $+6\%$ P_2/P_0 (pole hot) offset between the reemit and ignition targets for an ignition symmetric picket ($P_2/P_0 = 0$).

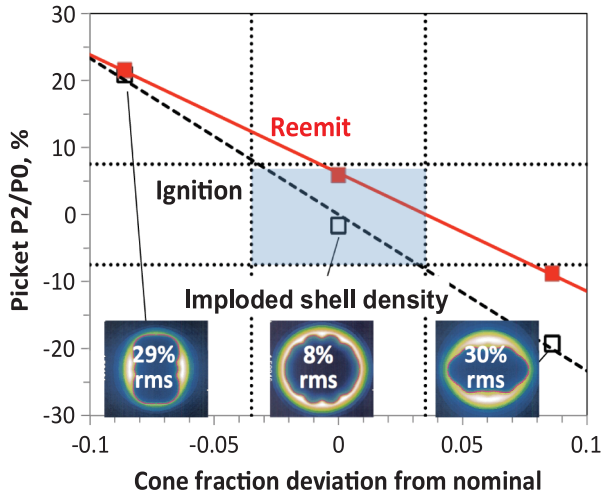


FIG. 2 (color). Calculated picket P_2/P_0 for reemit and ignition targets and imploded ignition core shell areal density cross section (hohlraum axis vertical) vs deviation from symmetric picket cone fraction (CF_0). Positive (negative) picket P_2 is pole (waist) hot asymmetry.

Figure 3 illustrates the experimentally inferred incident P_2/P_0 for reemit targets vs incident laser cone fraction CF_0 for two ignition hohlraum designs, referred to as scale 544 (5.44 mm diam \times 10.01 mm length) and 575 (5.75 mm diam \times 9.43 mm length). Also shown are the measured reemit images at 800 eV photon energy vs incident laser cone fraction for the scale 544 hohlraums.

The images and the P_2/P_0 measurements are taken at the time of maximum x-ray flux at the capsule (1.4–1.5 ns) that, according to calculations, is within ~ 0.1 ns of the maximum hohlraum x-ray flux measured by Dante [22] [Fig. 1(b)]. All variations of CF_0 were performed keeping the total power P_{tot} constant. The single black data point in Fig. 3 was obtained with no wavelength separation ($\Delta\lambda = 0$) between the inner and outer cones, a case in which our models predict no net CBET between the outer and the inner cones [23]. For the initial laser cone fraction of $CF_0 = 0.36$, the measured asymmetry in scale 575 was $P_2/P_0 = -5\%$, in close agreement with 3D HYDRA simulations (black dashed lines in Fig. 3). On the other hand, for the red data points, obtained with a wavelength separation $\Delta\lambda = 1.83$ Å between the inner and outer beams (typically used to achieve symmetric implosions using CBET during the fourth pulse) the laser cone fraction needs to be reduced by 0.24 and 0.2 for the target scales 544 and 575, respectively, in order to obtain the same P_2 symmetry. This demonstrates that when $\Delta\lambda$ is applied, CBET from the outer beams to the inner beams occurs, thus requiring a lower incident cone fraction to recover a symmetric x-ray drive.

The reemit tuning curves summarized here show that symmetry can be tuned to high precision during the picket even in the presence of strong CBET. The inferred P_2/P_0 has the expected linear dependence on CF_0 (solid line for scale 544 in Fig. 3) near $P_2/P_0 = 0$, and its variation from

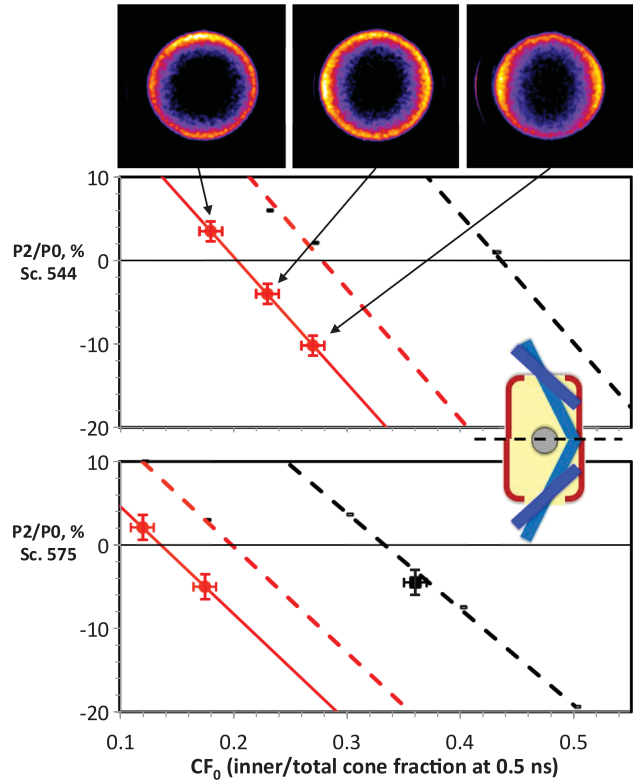


FIG. 3 (color). Inferred incident P_2/P_0 from experiments (points and solid lines) at peak x-ray drive [$t = 1.4$ ns (1.5 ns) for scale 544 (575) hohlraums] vs picket laser cone fraction CF_0 and HYDRA simulations with a linear CBET model (dashed lines). The black lines and single data point are for $\Delta\lambda = 0$ (no CBET), whereas the red data points and calculations are for $\Delta\lambda = 1.83$ Å. Experimental images (top) of the reemit capsule at the three CF_0 are also shown for the scale 544 hohlraums (hohlraum axis is vertical).

linearity is well within the 1% uncertainty that is dominated by the accuracy of the data photon statistics. Therefore the P_2/P_0 symmetry can be tuned to an accuracy that is much better than the $\pm 7.5\%$ requirement for ignition. Furthermore, the inferred symmetric picket cone fraction for ignition targets ($P_2 = 0$) at $\Delta\lambda = 1.83$ (0) Å are 0.16 and 0.1 (0.3) for scales 544 and 575 hohlraums, respectively, after accounting for ignition vs reemit targets offset $\Delta CF_{\text{ir}} = -0.04$ (Fig. 2). Recent dual axis shock timing experiments [24], which show nearly simultaneous (within ± 50 ps) breakout times of the first shock at the pole and equator, have confirmed that these cone fraction settings produce an early-time drive P_2/P_0 symmetry of $0 \pm 5\%$ in ignition targets.

Figure 4(a) shows the P_2/P_0 time history for two of the scale 575 experiments (Fig. 2) with $CF_0 = 0.18$, $\Delta\lambda = 1.83$ Å (red), and $CF_0 = 0.36$, $\Delta\lambda = 0$ (black). Since the time history of the picket P_2/P_0 asymmetry is essentially the same for these two experiments within the experimental accuracies, this implies that the cone fraction at the hohlraum wall was similar in both cases (with and without

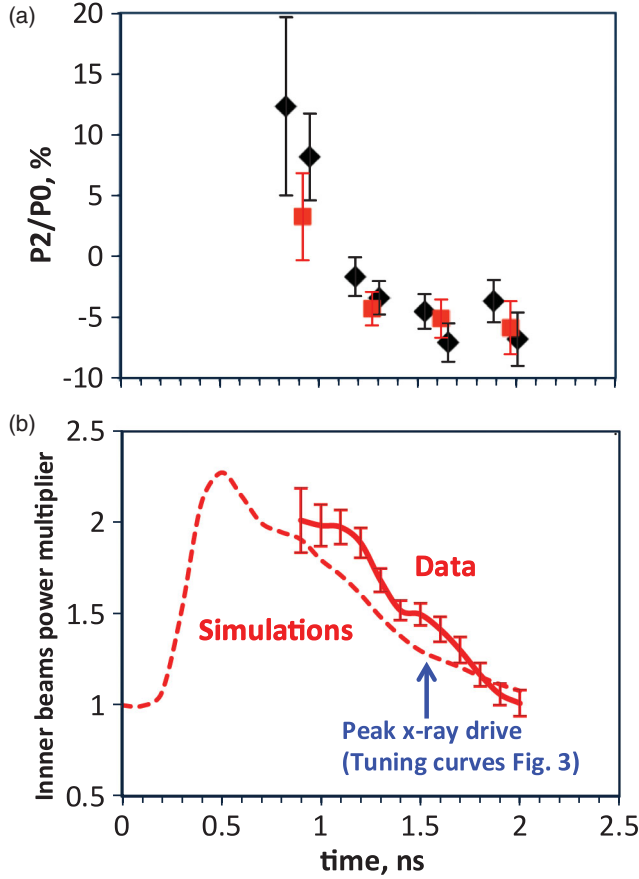


FIG. 4 (color). (a) Measured inferred incident P_2 vs time for $CF_0 = 0.36$ and $\Delta\lambda = 0$ (black solid diamonds) and for $CF_0 = 0.18$ and $\Delta\lambda = 1.83 \text{ \AA}$ (red solid squares). (b) inferred inner beam power increase from CBET for $CF_0 = 0.18/\Delta\lambda = 1.83 \text{ \AA}$ (red solid), and calculated from simulations (red dashed).

CBET). Under this assumption, since the total power $P_{\text{tot}}(t)$ was kept the same for both cases, we simply have $P_{\text{inn}}^{\Delta\lambda=0}(t) = P_{\text{inn}}^{\Delta\lambda=1.83 \text{ \AA}}(t) * \alpha_{\text{inn}}^{1.83 \text{ \AA}}(t)$, where $\alpha_{\text{inn}}^{1.83 \text{ \AA}}(t)$ is the inner beams power multiplier from CBET at $\Delta\lambda = 1.83 \text{ \AA}$, which can thus be estimated from the ratio of the inner beams powers or cone fractions.

This relation is valid for no CBET in the $\Delta\lambda = 0$ experiment, i.e., $\alpha_{\text{inn}}^{0 \text{ \AA}} = 1$, as suggested by the agreement between the black data point and calculations shown in Fig. 3 (Sc. 575). The time-resolved inner beam amplification from CBET inferred from the measured cone fraction ratio is shown in Fig. 4(b) (solid line). The error bars are derived from the accuracy in the P_2/P_0 measurements [Fig. 3(a)], since our assumption that the symmetry time histories are similar is only valid within this accuracy.

These results show strong early time CBET for $\Delta\lambda = 1.83 \text{ \AA}$, leading to inner beams multipliers of up to $2 \times$, even though the laser intensities are much lower in the picket ($I \sim 10^{13} \text{ W/cm}^2$ per quad) than during the fourth pulse ($I \sim 10^{14}\text{--}10^{15} \text{ W/cm}^2$), where comparable CBET multipliers were previously measured [11–13]. This can be

explained by the different plasma conditions between these two times at the laser entrance holes, where CBET is occurring [Fig. 1(c)]; the electron density is $2 \times$ higher in the picket ($n_e \sim 0.1n_c$, vs $0.05n_c$ during the fourth pulse— n_c is the critical density), and the electron temperature is also much lower ($T_e \sim 1 \text{ keV}$, vs $\sim 4 \text{ keV}$, respectively). Since the exponential amplification gain for the inner beams scales like $I_{\text{out}} * n_e/T_e$, where I_{out} is the outer beam intensity, the increase in n_e/T_e balances partially the $30 \times$ decrease in laser intensity. The plasma waves driven by $\Delta\lambda$ are also typically closer to the ion acoustic resonance during the picket, when the flows and the sound speed ($\propto T_e^{1/2}$) are smaller than during the fourth pulse. The ion heating process, which was recently identified as a possible CBET saturation mechanism during the fourth pulse [17,25], is not expected to play a role in the picket because the power deposited in the ion plasma waves is too small; our estimates show that the ion heating rates are of the order of 0.01 keV/ns in the picket, vs several keV/ns in the fourth pulse. The amplitude of the driven plasma waves is also too small ($\delta n/n \sim 10^{-4}$ for our conditions) to be subject to other saturation mechanisms.

As a result, the decrease in inner beams amplification in Fig. 4(b), validated experimentally by P_2/P_0 data between $t = 0.9$ and 2 ns , roughly follows the linear decrease of the outer beam power [Fig. 1(b)], indicating that CBET in the picket operates in a linear regime. Shock velocity data that are recorded at later times [9] confirm the time integrated effect of CBET in the picket, consistent with the present results.

The experimental data at $\Delta\lambda = 1.83 \text{ \AA}$, suggests 20% – 25% more picket CBET than calculated (Figs. 3 and 4) over the $0.9\text{--}2 \text{ ns}$ time interval where the measurements are performed. Since laser-plasma interactions (CBET, inverse Bremsstrahlung absorption) and radiation-hydrodynamics are highly correlated, the discrepancy in CBET could be due to modeling errors in either of these processes.

In summary, we have successfully demonstrated high precision tuning of the radiation P_2/P_0 symmetry during the picket of NIF ignition hohlraums laser pulses using reemit experiments. P_2/P_0 tuning was performed both in the presence of CBET (by using a wavelength separation between different cones of laser beams) as well as without CBET (with all the laser beams at the same wavelength). We demonstrated that the P_2/P_0 symmetry during the picket can be tuned to better than 1% accuracy even in the presence of strong CBET, well below the $\pm 7.5\%$ ignition requirement. Comparing experiments with and without CBET that resulted in the same measured symmetry allowed us to infer the time history of CBET during the picket. We show that the inner beams are amplified by more than a factor of 2 for a wavelength shift $\Delta\lambda = 1.83 \text{ \AA}$ required for time-integrated symmetry. Such strong CBET is possible because of higher densities and lower

temperatures in the crossing beam plasma region that occur during the picket as compared to that occurring during the fourth pulse of the ignition drive, even though the laser intensities are smaller by more than an order of magnitude. These measurements are in good agreement with fully three-dimensional simulations using the code HYDRA coupled to a linear CBET model, indicating that CBET operates in a linear, unsaturated regime during the picket.

This work was performed under the auspices of the U.S. Department of Energy by Lawrence Livermore National Laboratory under Contract No. DE-AC52-07NA27344.

-
- [1] G. H. Miller, E. I. Moses, and C. R. Wuest, *Nucl. Fusion* **44**, S228 (2004).
- [2] O. L. Landen, T. R. Boehly, D. K. Bradley, D. G. Braun, D. A. Callahan, P. M. Celliers, G. W. Collins, E. L. Dewald, L. Divol, S. H. Glenzer, A. Hamza, D. G. Hicks, N. Hoffman, N. Izumi, O. S. Jones, R. K. Kirkwood, G. A. Kyrala, P. Michel, J. Milovich, D. H. Munro, A. Nikroo, R. E. Olson, H. F. Robey, B. K. Spears, C. A. Thomas, S. V. Weber, D. C. Wilson, M. M. Marinak, L. J. Suter, B. A. Hammel, D. D. Meyerhofer, J. Atherton, J. Edwards, S. W. Haan, J. D. Lindl, B. J. MacGowan, and E. I. Moses, *Phys. Plasmas* **17**, 056301 (2010).
- [3] G. D. Tsakiris, J. Massen, R. Sigel, F. Lavarenne, R. Fedosejevs, J. Meyer-ter-Vehn, K. Eidmann, S. Witkowski, H. Nishimura, Y. Kato, H. Takabe, T. Endo, K. Kondo, H. Shiraga, S. Sakabe, T. Jitsuno, M. Takagi, C. Yamanaka, and S. Nakai, *Phys. Rev. A* **42**, 6188 (1990); W. A. Stygar, R. E. Olson, R. B. Spielman, and R. J. Leeper, *Phys. Rev. E* **64**, 026410 (2001).
- [4] F. Phillippe, A. Casner, T. Caillaud, O. Landoas, M. C. Monteil, S. Liberatore, H. S. Park, P. Amendt, H. Robey, C. Sorce, C. K. Li, F. Seguin, M. Rosenberg, R. Petrasso, V. Glebov, and C. Stoeckl, *Phys. Rev. Lett.* **104**, 035004 (2010).
- [5] J. D. Lindl, P. Amendt, R. L. Berger, S. G. Glendinning, S. H. Glenzer, S. W. Haan, R. L. Kauffman, O. L. Landen, and L. J. Suter, *Phys. Plasmas* **11**, 339 (2004).
- [6] M. Murakami and J. Meyer-Ter-Vehn, *Nucl. Fusion* **31**, 1333 (1991).
- [7] M. Basko, *Phys. Plasmas* **3**, 4148 (1996).
- [8] G. A. Kyrala *et al.*, *Phys. Plasmas* **18**, 056307 (2011).
- [9] H. F. Robey *et al.*, *Phys. Plasmas* **19**, 042706 (2012).
- [10] D. Callahan and J. Edwards, APS Report No. DPP.UO3.1, 2007.
- [11] P. Michel, L. Divol, E. A. Williams, S. Weber, C. A. Thomas, D. A. Callahan, S. W. Haan, J. D. Salmonson, S. Dixit, D. E. Hinkel, M. J. Edwards, B. J. MacGowan, J. D. Lindl, S. H. Glenzer, and L. J. Suter, *Phys. Rev. Lett.* **102**, 025004 (2009); P. Michel, L. Divol, E. A. Williams, C. A. Thomas, D. A. Callahan, S. Weber, S. W. Haan, J. D. Salmonson, N. B. Meezan, O. L. Landen, S. Dixit, D. E. Hinkel, M. J. Edwards, B. J. MacGowan, J. D. Lindl, S. H. Glenzer, and L. J. Suter, *Phys. Plasmas* **16**, 042702 (2009).
- [12] P. Michel, S. H. Glenzer, L. Divol, D. K. Bradley, D. Callahan, S. Dixit, S. Glenn, D. Hinkel, R. K. Kirkwood, J. L. Kline, W. L. Kruer, G. A. Kyrala, S. Le Pape, N. B. Meezan, R. Town, K. Widmann, E. A. Williams, B. J. MacGowan, J. L. Lindl, and L. J. Suter, *Phys. Plasmas* **17**, 056305 (2010).
- [13] S. H. Glenzer, B. J. MacGowan, P. Michel, N. B. Meezan, L. J. Suter, S. N. Dixit, J. L. Kline, G. A. Kyrala, D. K. Bradley, D. A. Callahan, E. L. Dewald, L. Divol, E. Dzenitis, M. J. Edwards, A. V. Hamza, C. A. Haynam, D. E. Hinkel, D. H. Kalantar, J. D. Kilkenny, O. L. Landen, J. D. Lindl, S. LePape, J. D. Moody, A. Nikroo, T. Parham, M. B. Schneider, R. P. J. Town, P. Wegner, K. Widmann, P. Whitman, B. K. F. Young, B. Van Wonterghem, L. J. Atherton, and E. I. Moses, *Science* **327**, 1228 (2010); J. D. Moody, P. Michel, L. Divol, R. L. Berger, E. Bond, D. K. Bradley, D. A. Callahan, E. L. Dewald, S. Dixit, M. J. Edwards, S. Glenn, A. Hamza, C. Haynam, D. E. Hinkel, N. Izumi, O. Jones, J. D. Kilkenny, R. K. Kirkwood, J. L. Kline, W. L. Kruer, G. A. Kyrala, O. L. Landen, S. LePape, J. D. Lindl, B. J. MacGowan, N. B. Meezan, A. Nikroo, M. D. Rosen, M. B. Schneider, D. J. Strozzi, L. J. Suter, C. A. Thomas, R. P. J. Town, K. Widmann, E. A. Williams, L. J. Atherton, S. H. Glenzer, and E. I. Moses, *Nat. Phys.* **8**, 344 (2012).
- [14] J. D. Lindl, Comments Plasma Phys. Control. Fusion **17**, 221 (1996).
- [15] J. L. Milovich, M. Edwards, and H. Robey, APS Report No. DPP.GO5.8, 2008.
- [16] M. M. Marinak, G. D. Kerbel, N. A. Gentile, T. R. Dittrich, and S. W. Haan, *Phys. Plasmas* **8**, 2275 (2001).
- [17] P. Michel, W. Rozmus, E. A. Williams, L. Divol, R. L. Berger, S. H. Glenzer, and D. A. Callahan, *Phys. Plasmas* **20**, 056308 (2013).
- [18] N. D. Delamater, G. R. Magelssen, and A. A. Hauer, *Phys. Rev. E* **53**, 5240 (1996); N. Delamater, P. Bradley, G. Magelssen, and D. Wilson, *Rev. Sci. Instrum.* **77**, 10E302 (2006); E. L. Dewald, C. Thomas, J. Milovich, J. Edwards, C. Sorce, R. Kirkwood, D. Meeker, O. Jones, N. Izumi, and O. L. Landen, *Rev. Sci. Instrum.* **79**, 10E903 (2008).
- [19] G. A. Rochau, J. E. Bailey, G. A. Chandler, T. J. Nash, D. S. Nielsen, G. S. Dunham, O. F. Garcia, N. R. Joseph, J. W. Keister, M. J. Madlener, D. V. Morgan, K. J. Moy, and M. Wu, *Rev. Sci. Instrum.* **77**, 10E323 (2006); D. K. Bradley, P. M. Bell, J. D. Kilkenny, R. Hanks, O. Landen, P. A. Jaanimagi, P. W. Mckenty, and C. P. Verdon, *Rev. Sci. Instrum.* **63**, 4813 (1992).
- [20] E. Dewald, J. Milovich, C. Thomas, J. Kline, C. Sorce, S. Glenn, and O. L. Landen, *Phys. Plasmas* **18**, 092703 (2011).
- [21] J. M. Soures, R. L. McCrory, T. R. Boehly, R. S. Craxton, S. D. Jacobs, J. H. Kelly, T. J. Kessler, J. P. Knauer, R. L. Kremens, S. A. Kumpan, S. A. Letzring, W. D. Seka, R. W. Short, M. D. Skeldon, S. Skupsky, and C. P. Verdon, *Laser Part. Beams* **11**, 317 (1993).
- [22] E. L. Dewald, K. M. Campbell, R. E. Turner, J. P. Holder, O. L. Landen, S. H. Glenzer, R. L. Kauffman, L. J. Suter, M. Landon, M. Rhodes, and D. Lee, *Rev. Sci. Instrum.* **75**, 3759 (2004).
- [23] $\Delta\lambda = \lambda_{\text{inners}} - \lambda_{\text{outers}}$ is defined at the UV laser wavelength incident on target $\lambda_0 = 351$ nm.
- [24] D. Callahan *et al.*, *Phys. Plasmas* **19**, 056305 (2012).
- [25] P. Michel, W. Rozmus, E. A. Williams, L. Divol, R. L. Berger, R. P. J. Town, S. H. Glenzer, and D. A. Callahan, *Phys. Rev. Lett.* **109**, 195004 (2012).